Acta of Bioengineering and Biomechanics
Vol. 16, No. 2, 2014

Original paper
DOI: 10.5277/abb140213

Evaluation of contact characteristics of a patient-specific artificial dysplastic hip joint

IBRAHIM MUTLU[1]*, LEVENT UGUR[2], TALIP CELIK[1], LEVENT BULUC[3], UMIT SEFA MUEZZINOGLU[3], YASIN KISIOGLU[1]

[1] Department of Biomedical Engineering, Kocaeli University, Kocaeli, Turkey.
[2] Department of Automotive, Technical Science Vocational School, Amasya University, Amasya, Turkey.
[3] Department of Orthopaedics and Traumatology, Kocaeli University, Kocaeli, Turkey.

This study addresses the results of the experimental measurements for the contact surface areas and contact pressure distributions of a dysplastic hip joint. The hip joint consists of pelvis, proximal femur and artificial cartilages for both acetabulum and femoral head. The dysplastic hip joint is modeled in three dimensional (3D) form using the computerized tomography (CT) images obtained *in vivo* of an adult female patient. The modeled hip joint components are manufactured as a non-natural dysplastic hip joint using different materials and manufacturing processes. The dysplastic hip joint produced is subjected to compression forces experimentally to measure the contact surface area and contact pressure distributions between the femoral head and acetabulum using the pressure sensitive Fuji film. Different types of specific fixtures and molds are designed and manufactured to produce the dysplastic hip joint components and perform the experimental studies. The measured results using a non-natural dysplastic hip joint are compared with relevant results reported in current literature considering the peak and mean contact pressure values. Therefore, the obtained results showed that the non-natural dysplastic hip models can be generated and replaced to determine the contact characteristics for an elusive cadaveric model. In conclusion, the artificial models might be useful to understand the contact pressure distributions and potential changes in surface pressure contours and their effects on the stress distributions.

Key words: *biomechanics, pressure, hip dysplasia*

1. Introduction

The hip dysplasia is described by an irregular relation between the femoral head and the acetabulum. Insufficient coverage of the femoral head by the acetabulum leads to the development of dysplasia in the hip joint. The stresses and pressure distributions usually change with coverage angle of the femoral head in the articular surface of hip joint [1]–[5]. A nonuniform pressure or stress distribution in the dysplasia could play an important role in osteoarthritis process [6], [7] and lubrication [8]. Measurements of the stress distribution, pressure and contact area of the hip joint can be determined by different approaches, broadly experimental and commonly numerical used by the researcher. Experimental studies are conducted with generally cadaveric [9]–[11] or/and sometimes artificial models of the hip joint [12]–[14] in their experimental studies based upon *in vivo* conditions. However, obtaining the cadaveric samples is generally difficult for experimental studies. Especially, it is almost unavailable to obtain the samples for specific animal or cadaveric studies, having disorder of the patient such as hip dysplasia. Hence, the artificial models are sometimes used in the research [12]–[18].

Studies show, in particular, that the contact characteristics analyses of the specific dysplastic hip joints are inadequate even in few studies presenting contact stresses in normal and dyspalstic hip joints. Although

* Corresponding author: Ibrahim Mutlu, Department of Biomedical Engineering, Kocaeli University, Umuttepe Campus, 41380, Kocaeli, Turkey. Tel: +90 262 303 23 28, fax: +90 262 303 23 29, e-mail: ibrahim.mutlu@kocaeli.edu.tr

Received: July 30th, 2013
Accepted for publication: November 18th, 2013

comparisons between experimental and analytical methods for hip dysplastic model were reported [12], and the validations between experimental and finite element studies were made for the healthy hip joints [19]. Specific artificial models can also provide insight patient information, medical illustrations [20] and allow investigating the influence of pelvis osteotomy [13].

In this study, contact pressure and area of the hip joint were measured experimentally using the produced artificial model. A specific biomodel of the dysplastic hip joint including proximal femur and acetabular dysplastic pelvis were modeled and manufactured artificially using the CT data obtained *in vivo* from a young adult female patient. In addition, the work is concerned with model availability for experimental studies in comparison with cadaveric or animal models. Therefore, the usability of the artificial model instead of cadaveric model is validated experimentally in viewpoints of biomechanical studies.

2. Material and methods

2.1. Modeling dysplastic hip joint

A female patient with acetabular dysplasia, 28 years old and 60 kg in weight, was scanned using a Toshiba Aquilion CT scanner at Kocaeli University Hospital to obtain her CT images. These images are exported into the computer in DICOM format within the pixel resolution of 512 × 512 along with 135 Kv and scanned slice thickness of 0.3 mm. Thresholding technique based on the Hounsfield Units (HU) was used to separate the bones from soft tissues in MIMICS (R12.11) program. A three-dimensional (3D) reconstruction of the hip joint was developed after the region growing process (Fig. 1). The components of the dysplastic hip joint including pelvis and proximal femur were modeled in STL data format.

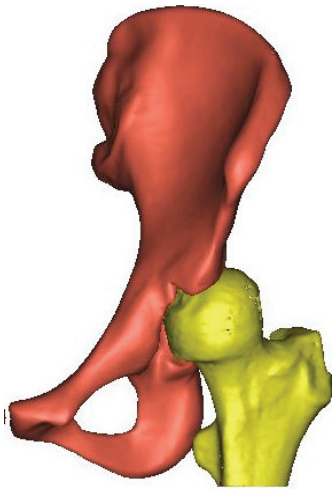

Fig. 1. The generated hip joint

2.2. Manufacturing total hip joint

The 3D computer model of dysplastic hip joint was obtained in STL format using CT images of the patient to convert the 3D computer aided design (CAD) model. The total hip joint including pelvis, proximal femur, articular cartilages of both acetabulum and femur head are manufactured using their 3D CAD models. The biomodel of the pelvis was manufactured by rapid prototyping 3D printer (Z-Corporation Spectrum Z510) using plaster-like powder through a Fused Deposition Modeling method [20] (Fig. 2). The pelvis model produced was augmented by vulcanized silicon molding technique to carry out plenty of tests. The pelvis model is molded using silicon material (Fig. 2). The artificial pelvis model manufactured by rapid prototyping 3D printer was used only to produce silicon mold for pelvis model. Twodozen of pelvis models were produced from polyurethane elastomer (Smooth-on Inch, PA, USA) [21] material using the molding process.

Fig. 2. The silicon mold and unilateral pelvis produced

The 3D proximal femur model converted from the CT images of the patients was imported into GEOMAGIC STUDIO, reverse engineering based CAD software. The software uses STL data to generate the 3D CAD models employing the Non-Uniform Rational B-

Splines (NURBS) surface type. The NURBS surface requires some process such as de-noising, smoothing, filling of gaps, removing spikes, repairing intersections to form CAD models. After generating the 3D smooth surface modeling, the 3D CAD model of the proximal femur was reconstructed. The reconstructed 3D proximal femur CAD model was manufactured using metal cutting process with five-axis computer aided numerical control milling machine (MIKRON HSM-400 5-axis) (Fig. 3a). The left proximal femur model was manufactured from aluminum alloy (Al 5083) material using a ball-nose end milling cutters with the ball-nose diameters of 20 mm, 10 mm and 5 mm, sequentially, to obtain smooth surface. The AL 5083 femur model was subjected to precise grinding and then sandblasting processes to obtain smoother and finish surface after the end milling process (Fig. 3b). After manufacturing the proximal femur model, a few artificial femur models were produced from polyester material by molding using the Al 5083 femur model (Fig. 3c). These models are used to produce articular cartilage models for the femoral head.

The use of articular cartilages in experimental studies is extremely important since the contact surfaces of the femoral head and acetabulum have irregular shapes so that pressure distributions were measured as non-uniform in the preliminary tests. Therefore, the articular cartilages of both acetabulum and femoral head were fabricated with non-uniform thicknesses by designing and modeling using CT images. In order to produce the articular cartilage models, two different 3D silicon molds were produced at room temperature. The cartilages for the femoral head and acetabulum were produced from the hot melt glue stick (HMGS) and RTV (room temperature vulcanized) silicone materials, respectively. The artificial cartilage produced was placed into the acetabulum of the artificial pelvis model using an adhesive material as shown in full cross-section of the acetabulum (Fig. 4a). The average layer thickness of the RTV artificial cartilage for the acetabulum cavity was measured as 2 mm. In order to create and produce the artificial cartilage for the femoral head, the Al 5083 femoral head model produced was used to form the silicon mold cavity.

a) b) c)

Fig. 3. The manufactured proximal femur models:
(a) Al 5083 femur model, (b) sandblasted model, (c) polyester femur model

a) b) c)

Fig. 4. The artificial cartilage models: (a) RTV-2 acetabulum cartilage, (b) HMGS femur head cartilage on the polyester model, and (c) HMGS femur head cartilage mounted on the Al 5083 femoral head model

The HMGS material was poured into the silicon mold cavity and then the polyester femoral head model produced was immersed immediately into the molten HMGS material using a metric guide to arrange the layer thickness of the cartilage. As seen the polyester femur model was pressed in the poured molten HMGS material to form the cartilage shape based on the femoral head (Fig. 4b). The artificial cartilage produced was mounted on the Al 5083 femoral head model after cooling process at room temperature (Fig. 4c).

2.3. Experimental study

The experimental equipment was designed and manufactured for the contact pressure measurements in this study. A hydraulic press with a capacity of 5 kN was used to apply the force caused by body weight. Different special equipment was designed and produced to hold the artificial dysplastic hip model on the workbench of the press in a position of regular standing (vertical) posture. A suitable special fixture was designed and manufactured from compressed wood material to hold the pelvis model on the workbench. The fixture consisting of bilateral parts was manufactured in the shape of sacroiliac joint surface of the pelvis model (Fig. 5). The irregular surfaces of the fixture were modeled using the surface model of the pelvis. The surfaces of the fixture parts were machined using end milling machine. In the milling machine, different sizes of ball-nose end mills are used considering the different processing parameters to obtain smooth irregular surfaces to grasp the sacroiliac surface shown with A in Fig. 5. The pelvis was fixed to a rotational clamp using the wood fixture. Alignment accuracy of the assembly based on main axes was controlled with bubble level scale. The femur and pelvis models were mounted on the hydraulic press workbench (Fig. 6). The femur was positioned considering standing position. A load cell having a ton capacity was attached between the press base-plate and the femur. Pressure sensitive film (Fuji Photo Film Co., Ltd., Japan) was prepared in rosette form and sealed using stretch film and inserted on the artificial cartilage of the femur head. The sensitive films were located and positioned in the defined a preliminary direction and location. The pressure sensitive films were used to measure the contact pressures by compressing between the articular cartilages of both femur head and pelvis acetabulum.

A compression force of 80 ± 2 kgf with a pressure sensitive film loading rate procedure was applied considering single leg stance in the tests. The experiments were performed within the environmental conditions of %40 ± 5 Rh humidity and 18 ± 1 °C temperature. The colored stains in different levels occurred on the pressure sensitive films after compressing tests based on the contact distributions between the femur head and acetabulum. The colored films were scanned with a scanner (Mustek 1248UB), having a 600 × 600 dpi resolution to read and scale the pressure levels. The colored stains on the films were evaluated to calculate the contact pressures using the scanned data.

2.4. Mechanical properties of artificial cartilages

The mechanical properties of the articular cartilages made out of RTV silicone and HMGS materials used in this study were measured to compare with the values of the cartilages published in current literature. The mechanical property measurements of two different artificial cartilages were performed using uniaxial

Fig. 5. The fixture design for pelvis model

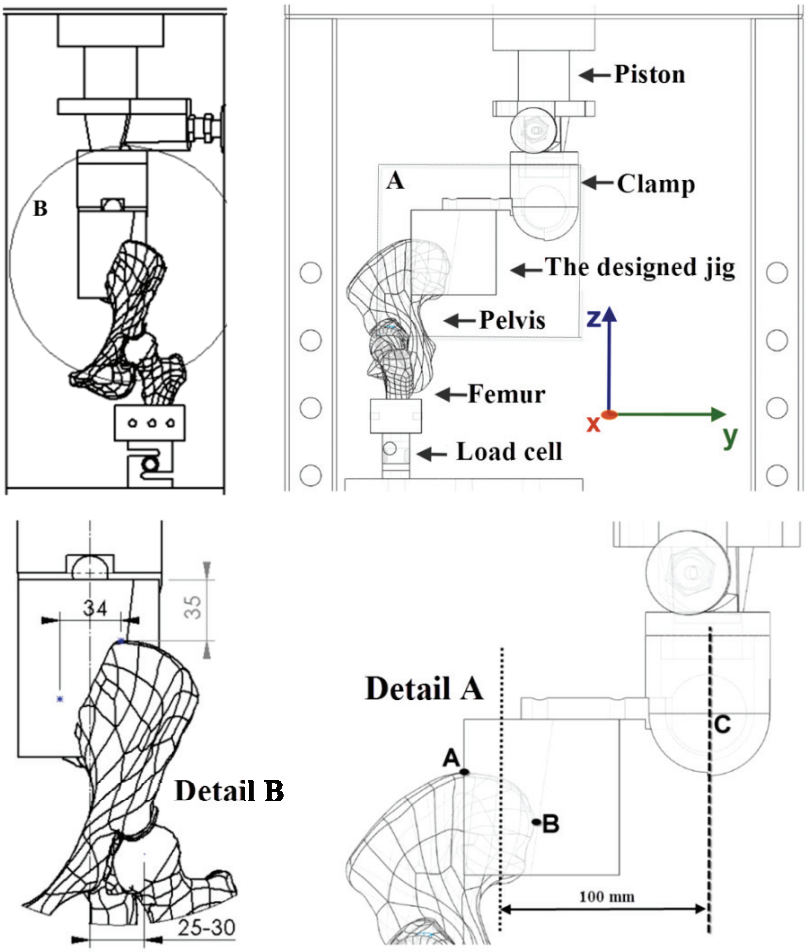

Fig. 6. Schematic view of the test rig

tensile test technique considering the ASTM D 412 standard requirements. This standard describes the test procedure of the vulcanized rubber and thermoplastic elastomers. The samples of the artificial cartilages for the tensile tests were prepared based on die C of ASTM standard to determine the non-natural cartilage properties. Engineering stress data for each sample is obtained as a function of corresponding engineering strains. The average values of the stress-strain data for ten samples were taken into account (Fig. 7). Two average stress-strain curves for both materials, RTV silicone and HMGS, used for the cartilages were obtained and plotted. In current literature, the stress-strain curves for natural articular cartilages were published being described as different types of materails such as linear elastic and hyperelastic materials. Young's modulus of linear elastic materials and shear modulus of neo-Hookean hyperelastic materials were given as E = 12 MPa [22]–[24] and G = 13.6 MPa [19], [25], respectively. Based on the material properties of both the RTV silicone and HMGS materials used in this study there were obtained lower than natural cartilage values. On the other hand, Young's modulus of artificial polyurethane elastomer pelvis (Task-9) and Al-5083 femur models used in this study was specified as 2.6 GPa and 72 GPa, respectively [21], [26]. The artificial materials are not similar to biological healthy bones of which the modulus of elasticity was reported as 17 GPa for cortical bones [27] and 0.12 GPa for cancellous bones [22].

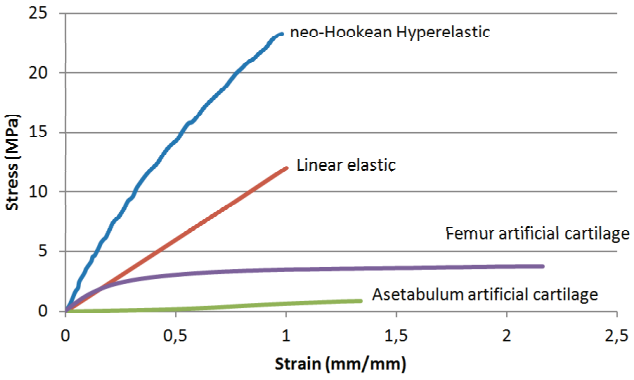

Fig. 7. Stress–strain curve of averaged uniaxial tensile test for hyperelastic and linear elastic cartilage and artificial cartilage materials: RTV mold silicone and HMGS

2.5. Measurement of contact pressure and area

Fujifilm prescale sensor, paper-based pressure sensitive film, was used in the tests to measure contact pressure and area of the hip joint. Low-grade pressure sensitive film with the capacity of 2.5–10 MPa was selected to measure the pressures. The calibration of the film was initially performed considering the widely used technique by Liggins et al. [28]. To calibrate the films, a steel punch polished and hardened with a diameter of 30 mm and polished metal plate surface were used to obtain uniform pressure distribution on the films. A spherical guide in a small spherical cavity on the punch was used to avoid eccentric loading effects during the tests. The tests were performed using the same hydraulic press having a ton capacity of load cell and the loads were applied in three steps with 5 second loading; increasing up to maximum value, held for 5 seconds and then released. The press load was applied to the samples within different magnitudes of 180, 270, 360, 450, 540, 630 and 720 kgf, to obtain different pressure distributions on the films as in colored stains. The films with colored red stains were scanned using the same scanner as mentioned above, with a 600 × 600 dpi resolution. The calibration tests were performed within the environmental conditions of %42 ± 3 Rh humidity and 19 ± 1 °C temperature.

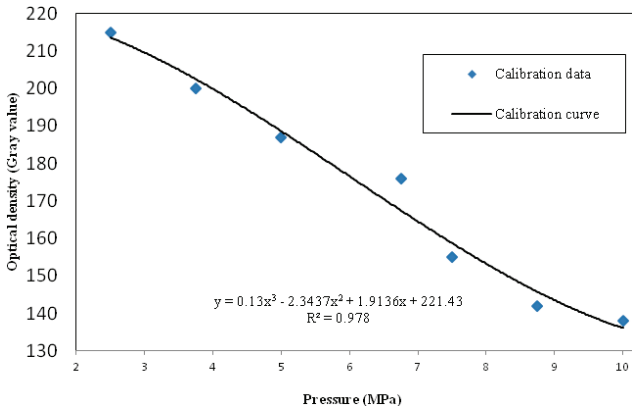

Fig. 8. Pressure sensitive film calibration curve

In order to evaluate the pressure distribution fairly, some undesired artifacts in the outer area of the scanned images were wiped out using eraser tool [29]. The images were converted to grayscale form using MATLAB software and then filtered in average value of 25 × 25 pixels to remove noises. The average values of the grayscale optical densities were considered except the pixels at the outer area and plotted with respect to the applied pressure. The calibration data of the optical density were plotted as a function of applied pressures and then regression analysis was used to generate the calibration curve (Fig. 8). The mid-values of the measured data from the samples were estimated with the calibration curve using the generated cubic polynomial equation.

3. Results

To evaluate the contact pressure distributions of a dysplastic hip joint, the scanned images of the pressure films with the colored stains were used to calculate the pressure values by employing the MATLAB program. The calculated contact pressure values are shown in Fig. 9 for three different cases of same loading scenario. As seen from the figure, the rosette forms of the films were positioned and placed on the femur head using SOLIDWORKS program with the same orientation used in the experiments to show the pressure distributions on the femoral head. Based on the colored pressure scales, the maximum pressure value was calculated as 10 MPa, which is also upper limit of low grade films. In addition, the contact areas and average contact pressure values of the artificial dysplastic hip joint used in this study were measured as 567.24–580.33-652.92 mm^2 and 3.01–2.86–2.67 MPa for three different cases, respectively.

4. Discussion

Many studies in literature have presented contact stresses in normal and dysplastic hip joints using both experimental and computer based numerical approaches. The purpose of these studies was to investigate the damage and degeneration limits of the cartilages and bones to determine the risks of aseptic and avascular necroses [30], [31]. The stresses in biological tissues play an important role in their regeneration [32]. The goal of this study was to measure the contact stresses and areas of a dysplastic hip joint utilizing the artificial models for conformity instead of cadaveric model.

The contact areas and pressure values were measured in variable position in this study since the stress distributions were non-uniform due to irregular contact surfaces. The peak pressure value was measured as 10 MPa in our studies using the low grade pressure films. Several studies presented also the peak press

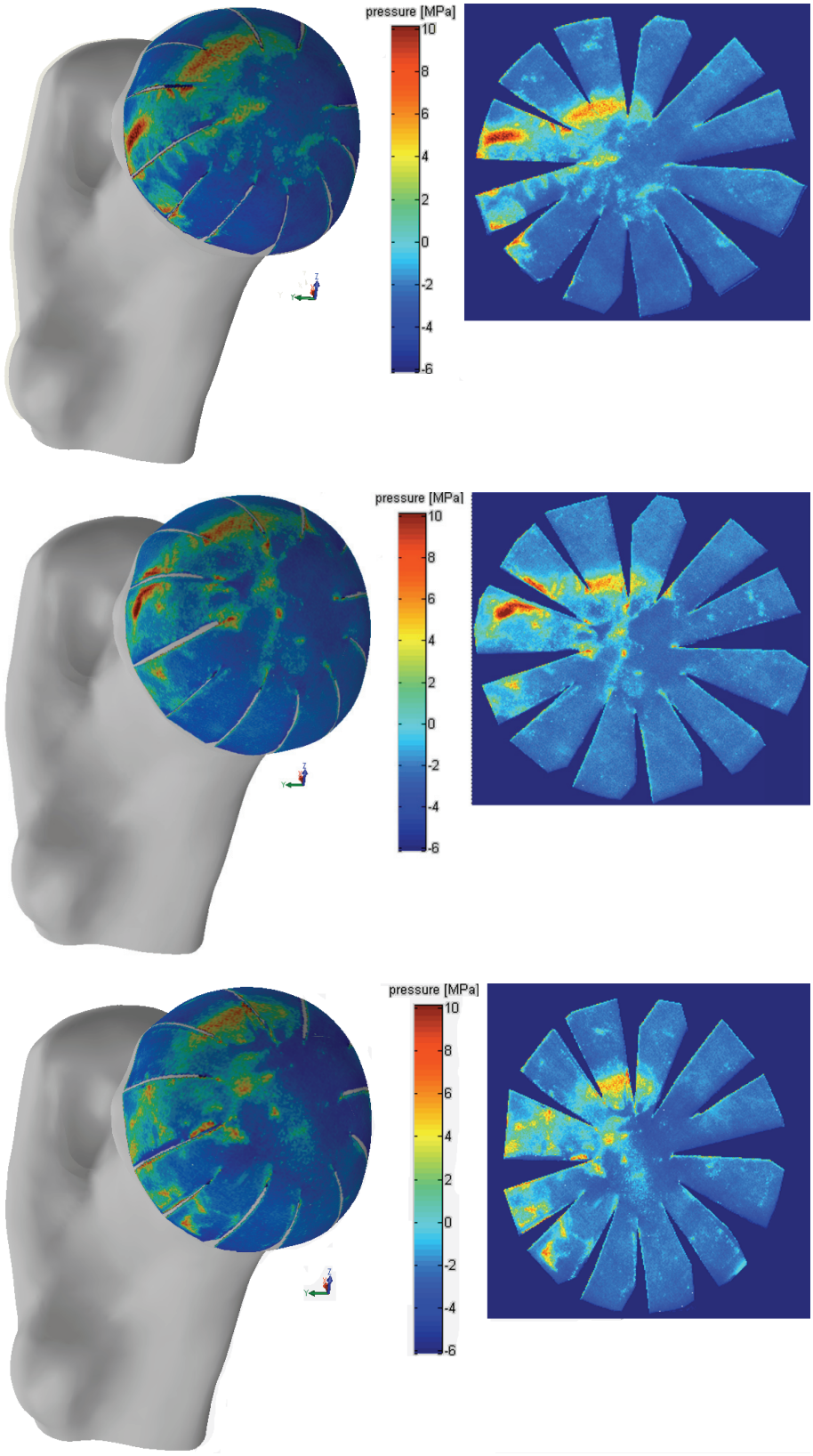

Fig. 9. The pressure distributions on the pressure sensitive films

values as 10 MPa at neutral position or mid-stance phase in the normal hip joints [9], [11], [19], [33], [34]. Afoke et al. presented different peak stress values as 8, 4.9 MPa [35], 6.2 MPa [9] in their different studies considering 1.33 times body weight in the normal hip joints. Konrath et al. [36], Olson et al. [33]

and von Eisenhart et al. [11] reported that peak stresses are measured approximately 6.2 ± 2.8, 8.08 ± 2.46 and 7.7±1.95 MPa in their normal hip joint models, respectively. Michaeli et al. [12] measured peak contact pressure approximately 6.65 ± 1.85 MPa using pressure load between 800–1200 N on the normal cadaveric hip joint. Therefore, the measured peak pressure values cannot be compared feasibly among these studies due to the low grade film capacity.

Konrath et al. [36], Olson et al. [33] and Anderson et al. [19] reported that the mean contact pressure values measured approximately 3.8 ± 0.95, 4.2 ± 1.1 and 4.7 ± 0.5 MPa, respectively, for mid-stance phase in their experimental studies. The contact pressure in literature was calculated using cadaveric normal hip joints. Based on these studies, the magnitudes of peak and mean pressures were presented in the range of 5–10 MPa which is acceptable for normal hip joints. The magnitudes of the peak and mean pressure values in our experiments are anticipated higher since the dysplastic hip joint model was used. But the mean pressure value was measured lower than in current literature, since the contact area of the dysplastic hip joint is smaller than the normal hip joint model, used in literature [19], [33], [36]. Therefore the maximum pressure value is obtained locally for the small contact areas in this study (see Fig. 9).

On the other hand, the contact pressure for a normal hip joint was calculated using finite element based approaches. Russell et al. [22], Bachtar et al. [37] and Anderson et al. [19] have calculated the maximum pressures during walking as 1.89 MPa, 5.50 MPa and 10.78 MPa, respectively. Russell et al. [22] and Anderson et al. [19] calculated the contact areas as 2265 and 304.2 mm^2, respectively. Russell et al. [22] studied only dysplastic hip joint using finite element method and calculated the maximum contact pressure as 6.73 ± 3.15 MPa and contact area as 614 ± 183 mm^2. Therefore, there is no measurement of mean pressure values for a dysplastic hip joints reported in current literature.

In current literature, there are two experimental studies that have been performed to determine the contact pressure with artificial hip joints. Iliescu et al. [38] measured and presented the contact pressure and the stress distribution in normal and dysplastic hip joints with the use of photoelasticity method. The cartilages and bones of the hip joint were manufactured from soft rubber and epoxy resin materials, respectively [38]. They measured peak pressure values for the normal and dysplastic hip as 8 MPa and 13.5 MPa, respectively. Michaeli et al. [12] measured contact pressures in their artificial hip biomodels and predicted peak contact stress of both normal and dysplastic hip joints to compare the experimental results. They measured the peak stresses in the artificial models approximately 0.825 ± 0.32 MPa applying 250 N static forces using the artificial hip models. Their calculation of the pressure values for both normal and dysplastic models was performed numerically for daily living activities. It is very difficult to draw a clear comparison from these two studies, since Iliescu et al. [38] used photoelastic models in 2D anteroposterior view of hip joint and Michaeli et al. [12] obtained experimental results with a ratio scale.

There are two main important factors affecting the contact characteristics, one is the geometry of contact surfaces and the other one is material stiffness. The magnitudes of contact pressures and areas measured from the tests of the artificial hip joints are highly dependent on the material properties of the cartilages. The material properties different than biological tissues are shown in Fig. 7 to clarify the questionable reasoning of the sample selections for the experiments. Young's modulus of the artificial cartilages (see Fig. 7) was measured lower than the articular cartilage values that causes lower contact pressures and higher contact areas. For a reasonable evaluation of the measured results, equivalent material mechanical properties with articular cartilages should be used in the studies, e.g., Iliescu [38] used articular cartilages having similar material properties.

From these studies, the peak values of the contact pressures were generally calculated in the range of 5–10 MPa even though the contact pressures were calculated analytically for the dysplastic hip. The explanation of the dysplastic hip behavior is highly dependent on the contact surface characteristics. It is evidently required that the contact characteristic determination is to reveal the dysplastic hip behavior since no report is available in literature about contact characteristics of the hip dysplasia.

Prescale-pressure sensitive film is a valuable tool to measure both contact areas and pressure distributions between the contact surfaces in particular biomechanical studies with an accuracy of 10% [39]. Also the contact areas and pressure values of pressure sensitive films can be determined less than 10% of accurate results using the image processes [40]. In addition, inserting the pressure sensitive film alters the contact circumstances [41]. The covering of the pressure sensitive film on contact surfaces via stretch film affects significantly the film's response [42]. These findings should not be ignored in evaluating the results when using the prescale-pressure sensitive film for the measurements of the contact characteristics.

Validation of the artificial model used in our experiments is required to determine the usability for the

contact characteristics. In current literature, Anderson et al. [19] studied the validation of their cadaveric hip model using both experimental and finite element analysis. Michaeli et al. [12] used artificial hip model to compare the analytical results with the corresponding experimental results within a correlation scale. On the other hand, three-dimensional biomodels can be used for many purposes such as medical illustrations, surgical planning, robotic applications regarding surgical assistance and design of new implants. Moreover, these models can gain new perspective for the treatment of patient disorder.

5. Conclusions

A dysplastic total hip joint was modeled in 3D form using the CT data obtained *in vivo* from a young adult female patient. The component of the dysplastic hip joint including pelvis, proximal femur and cartilages for both acetabulum and femoral head were produced using different materials and manufactured considering the generated 3D computerized model of the hip joint. The artificial hip model produced was tested experimentally to measure the contact surface areas and contact pressure distributions. In order to test the dysplastic hip model in a hydraulic press, specific fixture equipment was designed and manufactured to control the pelvis and proximal femoral head in a natural standing posture. The pressure sensitive film was used to measure the contact surface areas and pressure distributions between the acetabulum and femoral head.

The confirmation of the methodology followed and offered bio-models used in this study that might suitably allow the analysis of contact phenomena in a degenerated hip dysplasia considering the relevant studies in current literature. In conclusion, the artificial dysplastic hip joint was modeled and produced successfully using the relative CT data since the measured contact surface area and contact pressure values were obtained reasonable. Therefore, the artificial models might be useful to understand the contact pressure distributions and potential changes in surface pressure contours and their effects on the stress distributions. In addition, the contact pressure distributions were calculated successfully by scanning the pressure sensitive films used in the tests.

Acknowledgements

This work was financially supported by the Scientific Research Projects Unit of Kocaeli University under the project number of 2010/099.

References

[1] WIBERG G., *Studies on Dysplastic Acetabula and Congenital Subluxation of the Hip Joint*, Acta Chir. Scand., 1939, 5, 135.

[2] LEGAL H., *Introduction to the biomechanics of the hip*, Springer-Verlag, Berlin, 1987.

[3] GENDA E., IWASAKI N., LI G., MACWILLIAMS B.A., BARRANCE P.J., CHAO E.Y., *Normal hip joint contact pressure distribution in single-leg standing-effect of gender and anatomic parameters*, J. Biomech. 2001, 34, 895–905.

[4] IGLIC A., KRALJ-IGLIC V., DANIEL M., MACEK-LEBAR A., *Computer determination of contact stress distribution and size of weight bearing area in the human hip joint*, Comput. Meth. Biomech. Biomed. Eng., 2002, 5, 185–192.

[5] MAVCIC B., POMPE B., ANTOLIC V., DANIEL M., IGLIC A., KRALJ-IGLIC V., *Mathematical estimation of stress distribution in normal and dysplastic human hips*, J. Orthop. Res., 2002, 20, 1025–1030.

[6] XU L., SU Y., KIENLE K.-P., HAYASHI D., GUERMAZI A., ZHANG J. et al., *Evaluation of radial distribution of cartilage degeneration and necessity of pre-contrast measurements using radial dGEMRIC in adults with acetabular dysplasia*, BMC Musculoskelet Disord., 2012, 13, 212.

[7] BRAND R.A., *Joint contact stress: A reasonable surrogate for biological processes?* Iowa Orthop. J. 2005, 25, 82.

[8] WIERZCHOLSKI K., *Stochastic impulsive pressure calculations for time dependent human hip joint lubrication*, Acta Bioeng. Biomech., 2012, 14, 81–100.

[9] AFOKE N.Y., BYERS P.D., HUTTON W.C., *Contact pressures in the human hip joint*, J. Bone Joint Surg. Br., 1987, 69, 536–541.

[10] SPARKS D.R., BEASON D.P., ETHERIDGE B.S., ALONSO J.E., EBERHARDT A.W., *Contact pressures in the flexed hip joint during lateral trochanteric loading*, J. Orthop. Res., 2005, 23, 359–366.

[11] VON EISENHART R., ADAM C., STEINLECHNER M., MÜLLER-GERBL M., ECKSTEIN F., *Quantitative determination of joint incongruity and pressure distribution during simulated gait and cartilage thickness in the human hip joint*, J. Orthop. Res., 1999, 17, 532–539.

[12] MICHAELI D.A., MURPHY S.B., HIPP J.A., *Comparison of predicted and measured contact pressures in normal and dysplastic hips*, Med. Eng. Phys., 1997, 19, 180–186.

[13] PRESSEL T., MAX S., PFEIFER R., OSTERMEIER S., WINDHAGEN H., HURSCHLER C., *A rapid prototyping model for biomechanical evaluation of pelvic osteotomies*, Biomed. Tech. (Berl)., 2008, 53, 65–69.

[14] ZANETTI E.M., BIGNARDI C., AUDENINO A.L., *Human pelvis loading rig for static and dynamic stress analysis*, Acta Bioeng. Biomech., 2012, 14, 61–66.

[15] JOHNSON E., YOUNG P., *On the use of a patient-specific rapid-prototyped model to simulate the response of the human head to impact and comparison with analytical and finite element models*, J. Biomech., 2005, 38, 39–45.

[16] DOBSON C.A., SISIAS G., PHILLIPS R., FAGAN M.J., LANGTON C.M., *Three dimensional stereolithography models of cancellous bone structures from *mCT data: testing and validation of finite element results*, Proc. Inst. Mech. Eng. H, J. Eng. Med., 2006, 220, 481–484.

[17] DHAKSHYANI R., NUKMAN Y., AZUAN A.O.N., *FDM models and FEA in dysplastic hip*, Rapid Prototyping J., 2012, 18, 215–221.

[18] PLOMINSKI J., WATRAL Z., KWIATKOWSKI K., *Testing the stability of the polyethylene acetabulum cemented on a frozen*

bone graft substrate on a model of an artificial hip joint, Acta Bioeng. Biomech., 2008, 10, 3–6.

[19] ANDERSON A.E., ELLIS B.J., MAAS S.A., PETERS C.L., WEISS J.A., *Validation of finite element predictions of cartilage contact pressure in the human hip joint*, J. Biomech. Eng., 2008, 130, 051008.

[20] DHAKSHYANI R., NUKMAN Y., OSMAN N.A., MERICAN A., GEORGE J., *Rapid prototyping medical models for dysplastic hip orthopaedic surgery*, Proc. Inst. Mech. Eng. H, J. Eng. Man., 2010, 224, 769–776.

[21] Task-9. SMOOTH-ON, Inc. PA, USA.

[22] RUSSELL M.E., SHIVANNA K.H., GROSLAND N.M., PEDERSEN D.R., *Cartilage Contact Pressure Elevations in Dysplastic Hips: A Chronic Overload Model*, J. Orthop. Surg. Res., 2006, 1, 6.

[23] ANDERSON D.D., GOLDSWORTHY J.K., LI W., JAMES RUDERT M., TOCHIGI Y., BROWN T.D., *Physical validation of a patient-specific contact finite element model of the ankle*, J. Biomech., 2007, 40, 1662–1669.

[24] CHEGINI S., BECK M., FERGUSON S.J., *The effects of impingement and dysplasia on stress distributions in the hip joint during sitting and walking: a finite element analysis*, J. Orthop. Res., 2009, 27, 195–201.

[25] HARRIS M.D., ANDERSON A.E., HENAK C.R., ELLIS B.J., PETERS C.L., WEISS J.A., *Finite element prediction of cartilage contact stresses in normal human hips*, J. Orthop. Res., 2012, 30, 1133–1139.

[26] Aluminum 5083 material properties, http://www.ozon.com/article.aspx?ArticleID=2804.2012. Ref. Type: Internet Communication.

[27] DALSTRA M., VAN ERNING L., HUISKES R., *Development and Validation of a Three-Dimensional Finite Element Model of the Pelvic Bone*, J. Biomech. Eng., 1995, 117, 272–278.

[28] LIGGINS A.B., STRANART J.C.E., FINLAY J.B., RORABECK C.H., *Calibration and Manipulation of Data from Fuji Pressure-Sensitive Film*, Clin. Asp. B, 1992, 3, 61–70.

[29] BACHUS K.N., DEMARCO A.L., JUDD K.T., HORWITZ D.S., BRODKE D.S., *Measuring contact area, force, and pressure for bioengineering applications: Using Fuji Film and Tek-Scan systems*, Med. Eng. Phys., 2006, 28, 483–488.

[30] HADLEY N.A., BROWN T.D., WEINSTEIN S.L., *The effects of contact pressure elevations and aseptic necrosis on the long-term outcome of congenital hip dislocation*, J. Orthop. Res., 1990, 8, 504–513.

[31] KRALJ-IGLIC V., DOLINAR D., IVANOVSKI M., LIST I., DANIEL M., MAVCIC B. et al., *Hip stress distribution may be a risk factor for avascular necrosis of femoral head*, [in:] T. Jarm, P. Kramar, A. Zupanic (eds.), 11th Mediterranean Conference on Medical and Biomedical Engineering and Computing, Springer, Berlin, Heidelberg, 2007, 282–285.

[32] HUISKES R., RONALD R., HARRY V.L.G., D. JJ. *Effects of mechanical forces on maintenance and adaptation of form in trabecular bone*, Nature, 2000, 405, 704.

[33] OLSON S., BAY B., CHAPMAN M., SHARKEY N., *Biomechanical consequences of fracture and repair of the posterior wall*, The Journal of bone and joint surgery, 1995, 77, 1184–1192.

[34] VON EISENHART-ROTHE R., ECKSTEIN F., MÜLLER-GERBL M., LANDGRAF J., ROCK C., PUTZ R., *Direct comparison of contact areas, contact stress and subchondral mineralization in human hip joint specimens*, Anatomy and embryology, 1997, 195, 279–288.

[35] AFOKE N., BYERS P., HUTTON W., *Tests on hypotheses about osteoarthritis and hip joints*, Ann. Rheum. Dis., 1992, 51, 485–488.

[36] KONRATH G.A., HAMEL A.J., GUERIN J., OLSON S.A., BAY B., SHARKEY N.A., *Biomechanical evaluation of impaction fractures of the femoral head*, J. Orthop. Trauma., 1999, 13, 407–413.

[37] BACHTAR F., CHEN X., HISADA T., *Finite element contact analysis of the hip joint*, Med. Bio. Eng. Comput., 2006, 44, 643–651.

[38] ILIESCU N., DAN PASTRAMA S., GRUIONU L.G., JIGA G., *Biomechanical changes of hip joint following different types of corrective osteotomy – photoelastic studies*. Acta Bioeng. Biomech., 2008, 10, 65–71.

[39] Fuji Photo Film Co. Ltd. Pressure measuring film-FUJI prescale film instruction manual.

[40] MURIUKI M.G., GILBERTSON L.G., HARNER C.D., *Characterization of the performance of a custom program for image processing of pressure sensitive film*, J. Biomech. Eng., 2009, 131, 14503.

[41] LIAU J.-J., HU C.-C., CHENG C.-K., HUANG C.-H., LO W.-H., *The influence of inserting a Fuji pressure sensitive film between the tibiofemoral joint of knee prosthesis on actual contact characteristics*, Clin. Biomech., 2001, 16, 160–166.

[42] LIGGINS A., SURRY K., FINLAY J., *Sealing Fuji Prescale pressure sensitive film for protection against fluid damage: the effect on its response*, Strain, 1995, 31, 57–62.